Pore-scale experimental investigation of in-situ wettability and displacement mechanisms governing WAG in oil-wet carbonates

Ziqiang Qin[1,*], *Maziar* Arshadi[1], and *Mohammad* Piri[1]

[1]Department of Petroleum Engineering, University of Wyoming, Laramie, Wyoming 82071, United States

Abstract. In oil-wet carbonates, due to low oil production through conventional waterflooding, water-alternating-gas (WAG) injection is deployed to enhance oil recovery. However, to date, there is a lack of fundamental understanding of the underlying physics governing the flow at the pore scale during WAG. The advent of advanced X-ray microtomography (micro-CT) technology provides opportunities to study this complex displacement process at the pore level. In this study, a series of miniature core-flooding experiments were performed at elevated temperature and pressure conditions, using a highly-accurate core-flooding system integrated with a high-resolution micro-CT scanner. Miniature core samples were subjected to a dynamic wettability alteration process (aging) with crude oil followed by three cycles of WAG injection. The samples were X-ray imaged to generate three-dimensional fluid occupancy maps during different two- and three-phase flow stages of the WAG cycles. Pore-scale displacement mechanisms governing WAG EOR under oil-wet conditions were examined by analyzing the pore-fluid occupancy maps. The results showed that WAG flooding scheme significantly enhanced oil recovery. The sweep efficiency of both gas and brine phases were increased due to the shielding effect of the trapped gas ganglia. Oil production diminished rapidly after two waterflooding and gas injection cycles.

1 Introduction

More than 60% of the world's oil resources are held in carbonates [1]. It is believed that carbonate rocks were initially water-wet. However, crude oil can rupture the water layer and alter the wettability of carbonate grains during aging [2]. Therefore, carbonate reservoirs commonly demonstrate an oil-wet condition. Buckley et al. [3] reported mechanisms of wettability alteration during the aging process including surface precipitation, oil polar component interactions, acid/base interactions, and ion binding.

Due to the preferential oil-wet states and the complex pore structure, conventional waterflooding usually results in low oil production in carbonates [4,5,6,7]. Various enhanced oil recovery (EOR) techniques were proposed to further produce the remaining oil left after waterflooding. One of the most common EOR methods in the oil industry is gas injection. In North America, gas injection schemes contribute to more than 60% of the ongoing EOR projects [8]. This technique has great potential applications because of its significantly higher displacement efficiency and relatively lower cost compared to those of other chemical-based EOR methods [9]. Moreover, to alleviate the negative effect of greenhouse gases on global climate, gas injection EOR projects could also serve as underground gas storage purposes (e.g., Carbon capture and storage).

The main technical limitation of continuous gas injection is the poor volumetric sweep efficiency due to the low viscosity and density of gas compared to those of other reservoir fluids [9]. Therefore, Water-Alternating-Gas (WAG) injection strategy was developed to manipulate the gas/oil mobility ratio. Furthermore, WAG injection could improve the vertical sweep efficiency as the migration of gas to the top and that of water to the bottom in reservoirs due to gravity.

In 1975, an immiscible CO_2-WAG project was conducted in Lick Creek Meakin Sand Unit, AR. It was reported that about 755 Mbbl additional oil was recovered due to the WAG injection [10]. Hsie and Moore [11] reviewed the performance of a miscible CO_2-WAG project in a U.S. gulf coast reservoir. The project achieved an additional oil recovery of 16.9% from a water-out Miocene reservoir in sixteen months. Masoner and Wackowski [12] showed the field-application results of a CO_2-WAG EOR project in Range Weber Sand Unit. 50% of the Unit's remaining oil was produced.

Huang and Holm [13] studied the performance of WAG injection in both water-wet and oil-wet Berea sandstones using core-flooding experiments. They concluded that more oil was trapped in the water-wet core compared to the oil-wet sample. Sohrabi et al. [14] conducted a series of WAG flooding experiments in micromodels. The results highlighted that WAG injection led to a higher oil recovery than continuous water or gas injections. Han and Gu [15] studied the effect of WAG slug ratio on oil recovery. They concluded that the optimum slug ratio was 1:1.

* Corresponding author: zqin@uwyo.edu

Even though numerous experimental studies have confirmed the effectiveness of WAG injection for EOR, the direct evidence obtained from naturally-occurring carbonate samples on pore-scale displacement mechanisms governing the observed recovery enhancements are scarce. The advent of X-ray microtomography (micro-CT) technology provides opportunities to study the pore-scale processes of this complex displacements. In the past decades, Micro-CT imaging technology has been used widely in the petroleum engineering area, such as in-situ contact angle measurements [16,17], three-dimensional fluid visualization [18], and local displacement pattern characterization [19]. Direct characterization of in-situ pore-fluid occupancy maps provides opportunities for investigating pore-scale displacement mechanisms. In this study, a series of miniature core-flooding experiments were performed at elevated temperature and pressure conditions, using a highly-accurate core-flooding system integrated with a high-resolution micro-CT scanner. Miniature core samples were subjected to a dynamic aging process with crude oil followed by three cycles of WAG injection. The samples were X-ray imaged to generate three-dimensional fluid occupancy maps during aging and different flow stages of the WAG cycles. Pore-scale displacement physics governing WAG injection under oil-wet conditions were examined by analysing the pore-fluid occupancy maps. To the best of our knowledge, this study is the first pore-scale experimental investigation of the afore-mentioned effects in naturally-occurring carbonates under reservoir conditions.

2 Experiments

2.1 Rock and fluid properties

The rock sample used in this study was a type of carbonate outcrops named Fond du Lac. We first drilled a 1.5 inch-in-diameter core plug and measured the porosity and permeability of the sample, yielding values of 10.45% and 119.6mD, respectively. Next, a miniature core sample, 4.9mm in diameter and 43.4mm in length, was drilled from the mother core using air as a coolant. The sample was dried at 110°C in an oven for 24 hours and cooled down to room temperature in a desiccator. The dry miniature sample was then scanned by a micro-CT scanner, and the absolute porosity of 10.2% was calculated based on image analysis.

Brine solution was synthesized based on a reservoir brine analysis report. In this study, formation brine and the brine used for first waterflooding shared the same composition. Brine was degassed for 1 hour before use. Crude oil was collected from an oil field located in the Permian Basin, Texas, USA. The oil was filtered through a 0.5 µm filter to remove any possible residue and debris. Then, the filtered oil was tagged with 13 vol% 1-iodooctane to enhance the X-ray attenuation contrast between fluids in the CT images. Commercial grade nitrogen (with a purity of 99.9%) was used for gas injection. Table 1 shows the details of brine and crude oil properties.

Table 1. Brine and crude oil properties

Fluids	Viscosity* (cP)	Density* (g/ml)	Salinity (ppm)	Asphaltene content(%)
Brine	0.74	1.01	25416	-
Crude oil	3.79	0.84	-	0.9

*The viscosity and density data were measured at 40 °C and ambient pressure.

2.2 Experimental apparatus

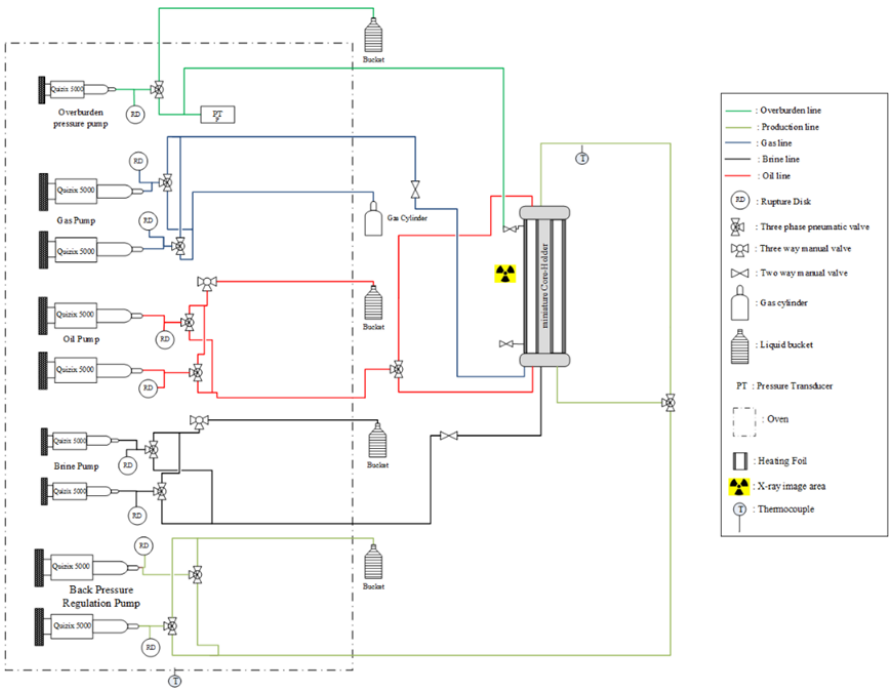

Fig. 1 A schematic diagram of the experimental apparatus [19].

The flow experiments were conducted using a three-phase reservoir-conditions core-flooding system integrated with a high-resolution X-ray micro-CT scanner. The core-flooding system consisted of five Quizix™ 5000 pumps (dual-cylinder with pressure and flow rate accuracies of 0.5 psi and 1.5* 10^{-5} cc/min), a custom-build core-holder, a series of Rosemount™ differential pressure transducers, heating and isolation units, and Hastelloy tubings to minimize corrosion. Three Quizix™ pumps were utilized to inject brine, oil, and gas into the core-holder. The overburden pump was used to maintain the confining pressure surrounding the core sample. The back pressure regulation pump received the fluids from the core-holder at constant pressure and subsequently discharged them into a beaker. The miniature core-holder was made out of carbon fiber to minimize the X-ray attenuation and was able to sustain a pressure and a temperature up to 7000 psi and 120°C, respectively. Highly flexible peek tubing was connected to the core-holder to minimize the vibration and torque during the scan process.

A Thermo Fisher heliscan micro-CT scanner was used to image the sample. The scanner consisted of an X-ray source, a sample stage, and an X-ray detector. The core-holder was mounted vertically inside the CT scanner and rotated during the imaging process. A number of projections were collected at different angles and reconstructed to generate three-dimensional maps of the rock and residing fluids during various stages of the experiment. A resolution of 700 nm to 64 µm was attainable depending on the magnification setting. The scanning parameters were appropriately chosen to maximize the signal-to-noise ratio and improve the quality of images (Table 2). Figure 1 illustrates a schematic of the experimental apparatus used in this study.

Table 2. X-ray microtomography parameters used in this study

X-ray current (uA)	X-ray voltage (kV)	Number of projections	Exposure time (s)	Voxel size (micron)	Scanning time (hours)
52.7	100	3600	0.42	2.37	3

2.3 Experimental procedure

The core sample was first placed inside the core-holder with a confining pressure of 300 psi. Gaseous CO_2 was injected into the core to remove the bulk air, and the system was subsequently vacuumed for 24 hours. The sample was then scanned to collect a set of reference images. Afterward, the vacuumed core sample was fully saturated with brine by injecting 50 pore volume of the fluid. Subsequently, the pore pressure and the confining pressure were simultaneously increased to 600 psi and 900 psi, respectively. The system temperature was also increased to 90°C by adjusting the thermo-controller of the heating tape surrounding the core holder. The temperature and pressure conditions were maintained at these values for the rest of experiments. The system was allowed to rest for five days to achieve an ionic equilibrium between the rock surface and the brine. The experiment was continued with a primary drainage step. Crude oil was injected into the sample with a constant flow rate of 0.006 cc/min. The core was continuously imaged during the primary drainage, and the steady state was confirmed until no change was observed in pore-fluid occupancy maps, i.e., after 10pv of oil injection (Figure 2). At this point, the initial brine saturation was calculated based on image analysis. The sample was then dynamically aged by injecting crude oil at a constant flow rate of 0.0002 cc/min. Scans was taken repeatedly during the aging process to monitor the evolution of in-situ oil-brine contact angles. The aging process was considered complete once the in-situ contact angles did not change further. The aging process produced an equilibrium wettability condition in approximately fifteen days (Figure 3). After completing the aging process, a waterflooding step with a flow rate of 0.0005 cc/min was performed. Then, the brine inside the sample was displaced by doped brine (by adding 18wt% NaI as tagging agent) at the same flow rate as the one used during waterflooding. This step aimed to ensure sufficient X-ray attenuate contrast existed among brine, oil, and gas phases during gas injection. A monitoring scan was taken to make sure the fluid occupancies did not change. Subsequently, a gas injection step was conducted at an injection rate of 0.015 cc/min. The low gas rate was chosen to ensure the flow in capillary dominated regime. The experiment was further continued with another two cycles of waterflooding (with doped brine) and gas injection alternatively to probe the pore-scale displacement mechanisms governing WAG injection. A series of scans were collected during the afore-mentioned flooding processes, and each flow step was terminated until the in-situ fluid occupancy map remained constant.

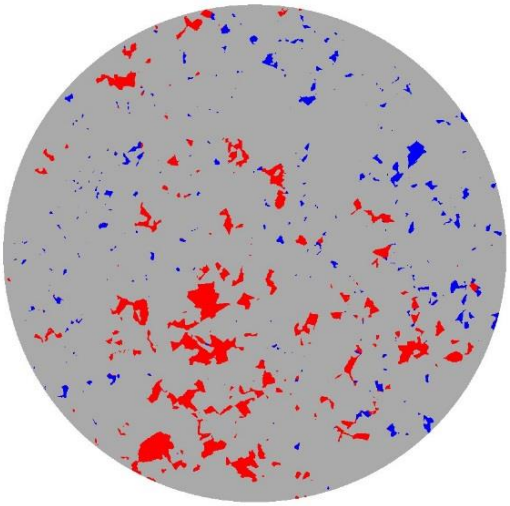

Fig. 2 Pore-fluid occupancy map at the end of the drainage process (grain: gray, oil: red, and brine: blue).

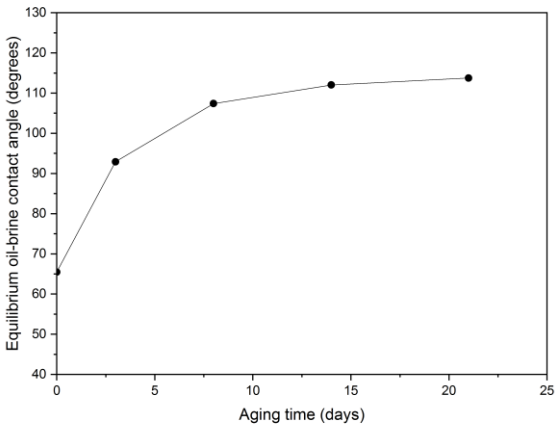

Fig. 3 Variation of equilibrium oil-brine contact angle versus aging time (Thirty contact angles were measured at each date point).

2.4 Data analysis

The middle part of the sample was scanned during the experiments to avoid any possible end effect. The bulk- and pore-volume in the field-of-view were 84.22 mm^3 and 8.6mm^3, respectively. The projections acquired during imaging processes were reconstructed to generate three-dimensional internal structures of the rock-fluid systems (with an image resolution of 2.37 micrometer). Avizo 9.4.0 and PerGeos 1.7.0 software platforms were used to analyse and visualize the acquired images. The first step of image-processing workflow was applying a volume edit module to mask the area out of region-of-interest. Then, a non-local means filter was used to smoothen the data and reduce noises. Afterward, the flooded image was registered to the dry reference image pixel-by-pixel. The registered wet image was subsequently multiplied by the pore map obtained from the dry image to eliminate the solid phase. Next, the multiplied image was segmented to various fluid phases. The segmented image was used to calculate fluid saturation, measure in-situ contact angles, characterize local displacement patterns, and perform other quantitative image analysis. The details of this robust image-processing workflow can be found elsewhere [19].

3 Results and Discussion

3.1 Pore-scale displacement mechanisms of WAG injection in oil-wet carbonates

In order to study the pore-scale displacement mechanisms during WAG injection in oil-wet carbonates, we performed a total of three water-gas injection cycles following the aging process. Before waterflooding, the initial brine saturation was 0.241. After aging, first, the sample was subjected to a waterflooding process. A significant amount of oil remained un-swept at the end of this stage, as shown in Figure 2a. The residual oil saturation (calculated from segmented pore-fluid occupancy maps) reached to 0.445, which translates to an oil recovery of 41.4%. Subsequently, the experiment was further continued with alternative cycles of gas injection and waterflooding. The pore-fluid occupancy maps of the first gas injection cycle revealed that no stable spreading oil layers were formed in the system (Figure 4). Furthermore, oil, brine, and gas were identified as wetting, intermediate-wetting, and non-wetting phases based on in-situ contact angle measurements. The details of the in-situ contact angle measurement method are presented elsewhere [19]. During the first gas injection, some oil was produced and the residual oil saturation reached to 0.284 (with a gas saturation of 0.55). We also observed that some portion of the unrecovered oil was pushed by gas to the water channels that were created in the first waterflooding while the rest of oil remained un-swept due to gas fingering.

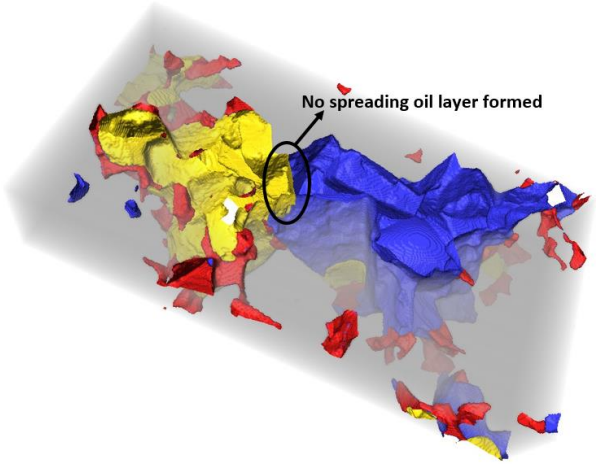

Fig.4 Exemplary three-dimensional pore-fluid occupancy map shows the spreading phenomenon in the system (grain: gray, gas: yellow, oil: red, and brine: blue).

As it can be seen from Figure 5 (a) and (c), during the second waterflooding cycle, brine mainly flowed through the channels filled with brine in the first waterflooding. However, there were also some new brine flow channels that were created during the second waterflooding. This is mainly because gas phase partially blocked some of the previously-invaded brine channels, which subsequently allowed brine to invade more pore elements and displace additional oil from the pore space. In addition, brine also displaced some of the gas into the oil-filled pores (Figure 5 (b) and (c)), which also benefited the oil production.

As shown in Figure 5 (b)-(d), gas flow channels of the second gas injection cycle could be divided into two groups. In the first category, the gas went through the previously-invaded gas channels created by the first gas injection. During this process, trapped gas globules were reconnected, and the oil occupying these channels could be produced. The second group was some new flow channels that were not invaded by gas during the first gas injection. The formation of these channels was due to the pressure build-up of the gas phase, which resulted from the shielding effect of fragmented fluid clusters that occupied the previously-invaded gas channels as more MTM interface were involved in the displacement chain. This pressure build-up facilitated the invasion of gas into

pore elements with high entry pressures. Consequently, some oil that was bypassed during the first gas injection was produced in this stage. Hence, the sweep efficiency of the gas phase was significantly increased in the second gas injection cycle compared to that in the first one, which is a crucial advantage of the WAG injection scheme.

The oil production diminished rapidly as the WAG cycles were continued. This is mainly due to two reasons: 1) the remaining oil was mostly located in small pores with high entry pressures. 2) The fluids' connectivity was very poor in this stage, which made the coalescence of the trapped oil difficult (The fluid connectivity was measured using axis connectivity module in Avizo 9.4.0).

The residual oil saturation after the first cycle of gas injection was 0.284 (with a gas saturation of 0.55), which corresponds to an additional oil recovery of 21.2%. For the second cycle of waterflooding and gas injection, the residual oil saturations were 0.188 (with a gas saturation of 0.4) and 0.122 (with a gas saturation of 0.77), which translates into the additional oil recovery of 12.6% and 8.7%, respectively. As for the third cycle, the residual oil saturations were 0.121 and 0.105, meaning the additional oil recovery of 0.1% and 2.1% (Figure 6). The pore-scale displacement mechanisms of WAG injection developed in this study could serve as a benchmark to improve the prediction capabilities of physically-based pore network models.

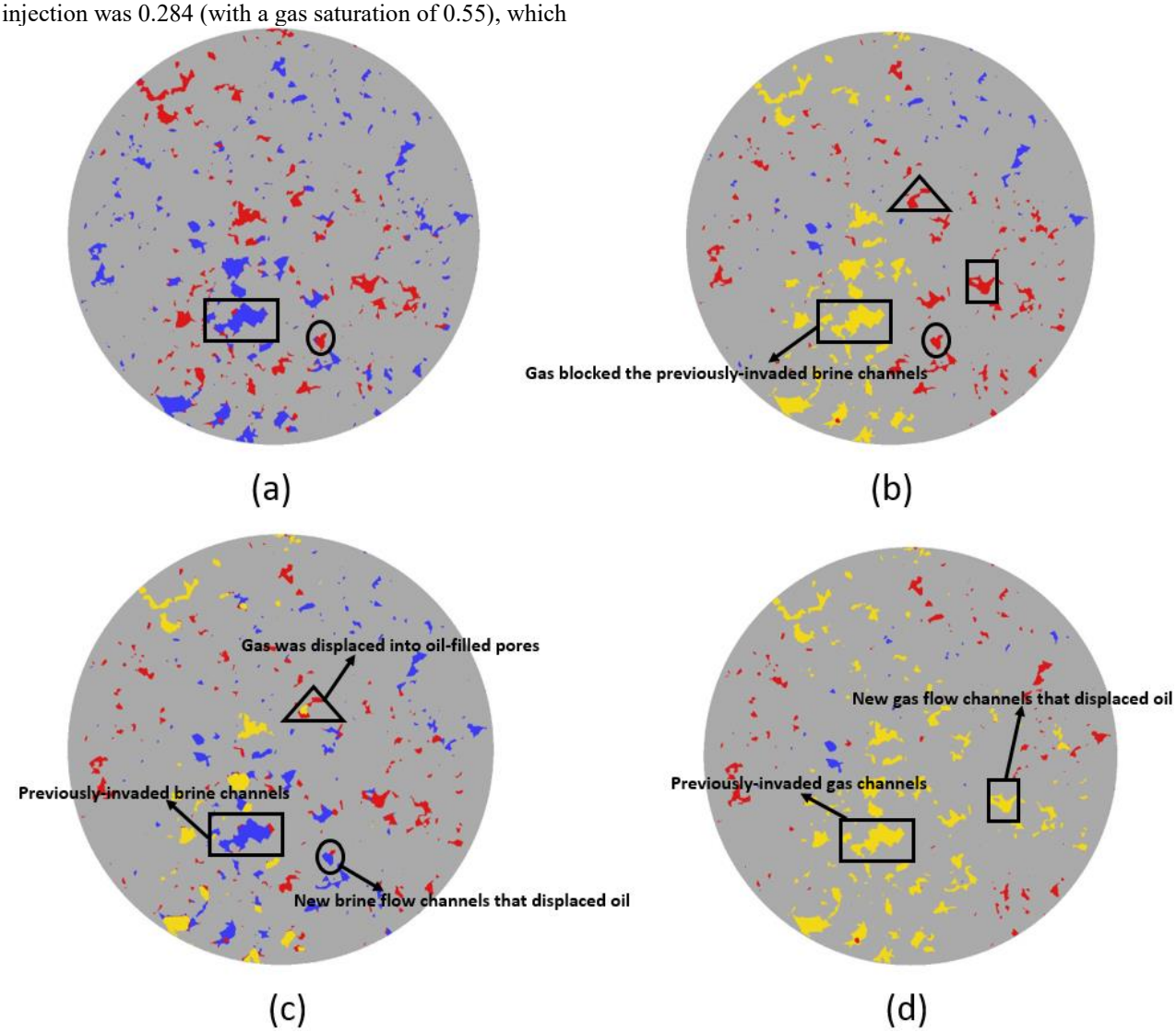

Fig. 5 Two-dimensional cross-sectional views of in-situ fluid occupancy maps at the end of (a) the first cycle of waterflooding, (b) the first cycle of gas injection, (c) the second cycle of waterflooding, and (d) the second cycle of gas injection (grain: gray, gas: yellow, oil: red, and brine: blue).

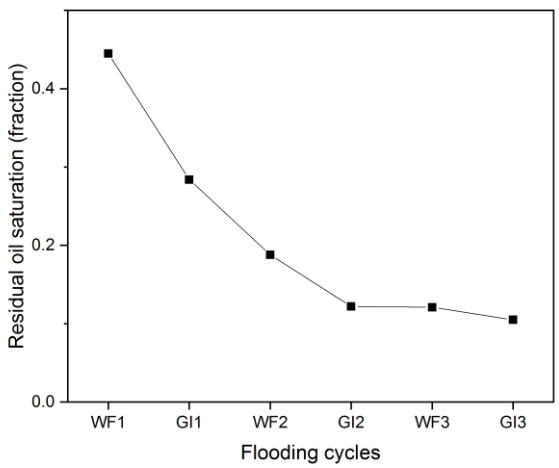

Fig. 6 Residual oil saturation at the end of varying WAG cycles (WF: waterflooding, GI: gas injection).

4 Summary and conclusion

In this study, a miniature core-flooding experiments were performed in naturally-occurring carbonate at elevated temperature and pressure conditions, using a highly-accurate core-flooding system integrated with a high-resolution X-ray micro-CT scanner. Pore-scale displacement mechanisms governing WAG injection under oil-wet conditions were investigated by analyzing the in-situ pore-fluid occupancy maps. Here, we summarize the main findings:

1) WAG flooding scheme significantly enhanced oil recovery. The oil saturation was ultimately reduced from 0.759 to 0.105 during this process.
2) WAG injection scheme remarkably increased the sweep efficiency of both gas and brine phases due to the shielding effect of the trapped fluid clusters.
3) After two waterflooding and gas injection cycles, the oil production diminished rapidly as the WAG cycles were further continued.

The authors gratefully acknowledge the financial support of Thermo Fisher Scientific Company, Hess Corporation, and the School of Energy Resources at the University of Wyoming.

References

1. Schlumberger, Carbonate reservoirs (2007).
2. N. R. Morrow, Wettability and its effect on oil recovery, Journal of Petroleum Technology **42**.12 (1990) 1–476.
3. J. Buckley, Y. Liu, and S. Monsterleet, Mechanisms of wetting alteration by crude oils, SPE journal **3**.01 (1998) 54–61.
4. J. Lai, et al. "Prediction of reservoir quality in carbonates via porosity spectrum from image logs." Journal of Petroleum Science and Engineering **173** (2019) 197-208.
5. J. Lai, et al. "Pore structure and fractal characteristics of Ordovician Majiagou carbonate reservoirs in Ordos Basin, China." AAPG Bulletin 20,190,412 (2019).
6. J. Lai, et al. "A review on pore structure characterization in tight sandstones." Earth-Science Reviews **177** (2018): 436-457.
7. W. Kuang, S. Saraji, and M. Piri. "A systematic experimental investigation on the synergistic effects of aqueous nanofluids on interfacial properties and their implications for enhanced oil recovery." Fuel **220** (2018) 849-870.
8. L. Koottungal, 2012 worldwide EOR survey, Oil & Gas Journal **110** (2012) 57–69.
9. Z. Qin, M. Arshadi, and M. Piri, "Micro-scale experimental investigations of multiphase flow in oil-wet carbonates. II. Tertiary gas injection and WAG" Fuel. (to be published)
10. T. B. Reid, and H. J. Robinson. "Lick creek meakin sand unit immiscible CO2 waterflood project." Journal of Petroleum Technology **33**.09 (1981) 1-723.
11. J.C. Hsie, and J. S. Moore. "The Quarantine Bay 4RC CO2 WAG pilot project: a postflood evaluation." *SPE reservoir engineering* **3**.03 (1988) 809-814.
12. R.K. Wackowski, and L. O. Masoner. "Rangely Weber Sand Unit CO2 Project Update: Operating History." *SPE Reservoir Engineering* **10**.03 (1995) 203-207.
13. E. T. S. Huang, and L. W. Holm. "Effect of WAG injection and rock wettability on oil recovery during CO2 flooding." *SPE Reservoir Engineering* **3**.01 (1988) 119-129.
14. M. Sohrabi, et al. "Visualization of oil recovery by water alternating gas (WAG) injection using high pressure micromodel-oil wet and mixed wet systems, SPE 71494." *Annual Technical Conference and Exhibition, New Orleans, Louisiana*. **Vol. 30**. (2001).
15. L. Han, and Y. Gu. "Optimization of miscible CO2 water-alternating-gas injection in the Bakken formation." Energy & Fuels **28**.11 (2014): 6811-6819.
16. M. Andrew, B. Bijeljic, and M. J. Blunt. "Pore-scale contact angle measurements at reservoir conditions using X-ray microtomography." Advances in Water Resources **68** (2014): 24-31.
17. H.H. Khanamiri, O. Torsæter, and J. Å. Stensen. "Effect of calcium in pore scale oil trapping by low-salinity water and surfactant enhanced oil recovery at strongly water-wet conditions: In situ imaging by X-ray microtomography." Energy & Fuels **30**.10 (2016): 8114-8124.
18. S. Youssef, et al. "4D imaging of fluid flow dynamics in natural porous media with ultra-fast X-ray microtomography." *International Symposium of the SCA, Napa Valley, California*. **Vol. 176**. 2013.
19. Z. Qin, M. Arshadi, and M. Piri, "Micro-scale experimental investigations of multiphase flow in oil-wet carbonates. I. In-situ wettability and low-salinity waterflooding" Fuel. (to be published)